Macromolecules
ARTICLE
pubs.acs.org/Macromolecules

Synthesis, Chiroptical Properties, and Photoresponsiveness of Optically Active Poly(*m*-phenyleneethynylene)s Containing Azobenzene Moieties

Hiromitsu Sogawa, Masashi Shiotsuki, Hideki Matsuoka, and Fumio Sanda*

Department of Polymer Chemistry, Graduate School of Engineering, Kyoto University, Katsura Campus, Nishikyo-ku, Kyoto 615-8510, Japan

Supporting Information

ABSTRACT: The Sonogashira–Hagihara coupling polymerization of 3′,5′-diiodo-4′-hydroxy-*N*-α-*tert*-butoxycarbonyl-D-phenylglycine ethyl-, hexyl-, and laurylamides **1a**–**c** with *p*-nonsubstituted, cyano, hexyl, and methoxy 3,5-diethynylazobenzenes **2a**–**d** was carried out to obtain optically active novel poly(*m*-phenyleneethynylene) with M_w values in the range from 6900 to 15 400 in 62–84% yields. CD and UV–vis spectroscopic data indicated that the polymers adopted thermally stable helical conformations in CH_2Cl_2 and *N,N*-dimethylformamide. Poly(**1b**–**2a**) further formed a chirally aggregated structure. The azobenzene moieties of the polymers underwent reversible photoisomerization upon UV- and visible-light irradiation, accompanying the changes of the higher-order structures.

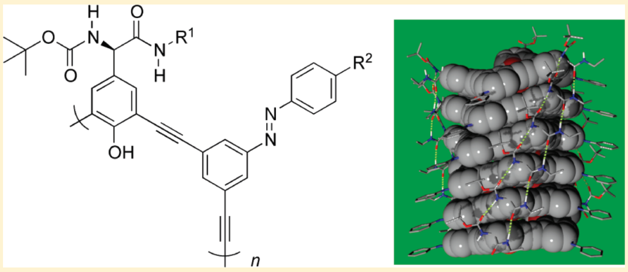

INTRODUCTION

Biomacromolecules such as proteins and DNA commonly have one-handed helical structures based on the homochirality of the components. Their functions and biological activities are generated by their well-defined higher-order structures. Artificial helical polymers have been extensively synthesized by imitating naturally derived helices.[1] The development of artificial helical polymers may encourage better understanding of the mechanisms for complicated and elegant functions of biopolymers. π-Conjugated helical polymers such as polyisocyanides,[2] polyacetylenes,[3] polythiophenes,[4] poly(phenylenevinylene)s,[5] and poly(phenyleneethynylene)s[6] have attracted much attention because of their potential of practical applications including molecular recognition materials,[7−12] chiral catalysts,[13−15] and chemical sensors[16−18] using their unique electronic and optical properties based on the secondary structures. Among them, poly(*m*-phenyleneethynylene)s substituted with polar groups tend to folded into helical structures in polar solvents based on the amphiphilic property between the hydrophilic side chains and hydrophobic main chain.[1b,19−21] We have recently found new examples of hydroxyphenylglycine- and tyrosine-based poly(*m*-phenyleneethynylene-*p*-phenyleneethynylene)s that adopt helical conformations consisting of hydrophobic exterior (alkyl groups and phenyleneethynylene main chain) and hydrophilic interior (hydroxy groups) in nonpolar solvents.[22,23] The helix formation of these polymers is based on the amphiphilic balance opposite from that of poly(*m*-phenyleneethynylene) derivatives reported so far.

Meanwhile, azobenzene is one of the best-known photoresponsive molecules undergoing reversible photoisomerization between trans and cis forms upon UV- and visible-light irradiation.[24] This conformational change triggers not only geometric change but also chemical properties such as dipole moment. Among various kinds of external stimuli, photoirradiation is practically useful for constructing sensing materials because of easy control over the irradiation wavelength, time, and intensity.[25−30] Azobenzene-containing π-conjugated helical polymers are applicable to intelligent materials that possess photoresponsiveness in addition to the electronic and optical properties, as mentioned above.[31−34]

Herein we wish to report the synthesis of novel hydroxyphenylglycine-derived poly(*m*-phenyleneethynylene)s containing azobenzene moieties (Scheme 1) and investigation of the effects of the alkyl chain lengths or substituent of azobenzene moieties on the higher-order structure, together with the solvent effect. We also report the reversible photoresponsive conformational changes of the polymers.

EXPERIMENTAL SECTION

Measurements. ^1H (400 MHz) and ^{13}C (100 MHz) NMR spectra were recorded on a JEOL EX-400 or a JEOL AL-400 spectrometer. IR spectra were measured on a JASCO FT/IR-4100 spectrophotometer. Melting points (mp) were measured on a Yanaco micro melting point apparatus. Elemental analysis was done at the Microanalytical Center of Kyoto University. Mass spectra were measured on an Applied Biosystems

Received: February 8, 2011
Revised: March 21, 2011
Published: April 08, 2011

dx.doi.org/10.1021/ma200281e | *Macromolecules* 2011, 44, 3338–3345

Scheme 1. Sonogashira–Hagihara Coupling Polymerization of Monomers 1a–c with 2a–d

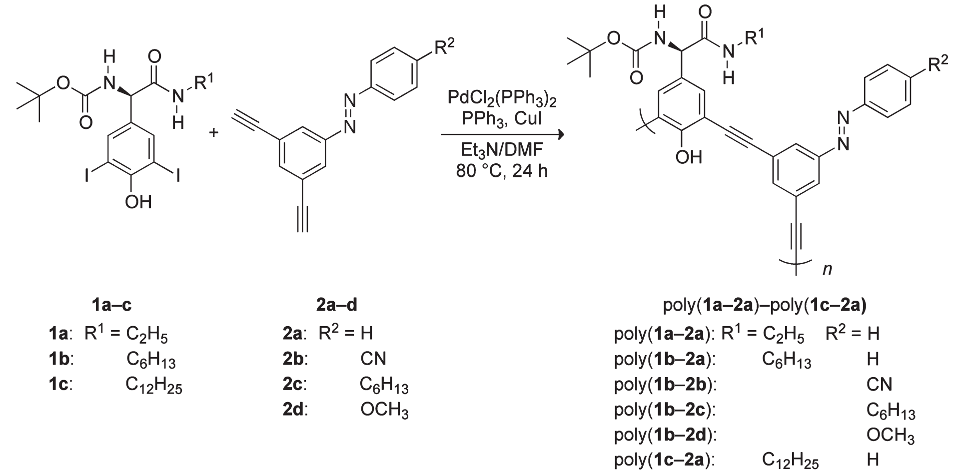

Scheme 2. Synthesis of Monomers 2a–d

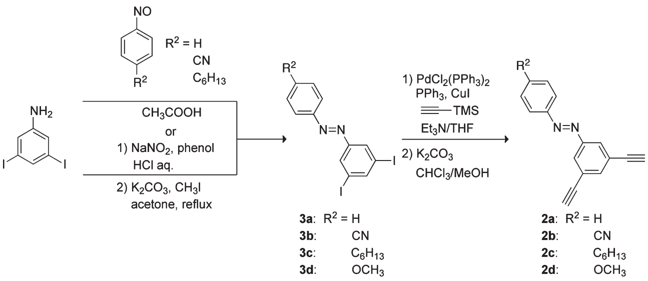

Voyager Elite MALDI mass spectrometer or a JEOL JMS-SX102A mass spectrometer. Number- and weight-average molecular weights (M_n and M_w) of polymers were determined by GPC (Shodex columns K803, K804, K805) eluted with CHCl$_3$ or (Shodex columns KF805 × 3) eluted with THF calibrated by polystyrene standards at 40 °C. CD and UV–vis absorption spectra were recorded on a JASCO J-820 spectropolarimeter. Dynamic light scattering (DLS) measurements were carried out with an Otsuka Electronic SLS-7000 goniometer with a GC-1000 correlator. The time-correlation functions were analyzed by double exponential methods. The measurements were performed at four different scattering angles, and the diffusion coefficient D was calculated from the slope of the straight line in the decay rate Γ versus q^2 plot, with q as the scattering vector. The hydrodynamic radii of scatterers were evaluated by the Stokes–Einstein equation.

Photoirradiation. Photoirradiation was carried out with a 400 W high-pressure mercury lamp equipped with a power source (HB-400, Fuji Glass Work) at room temperature. The appropriate wavelengths were selected either with a Pyrex glass and a UV-D33S filter (Toshiba) for irradiation at 300 nm < λ < 400 nm or with an L-42 filter (Toshiba) for irradiation at 420 nm < λ. Sample solutions were fed in a quartz cell, and it was placed 20 cm apart from the lamp. The photoisomerization was monitored by UV–vis absorption spectroscopy.

Materials. 3′,5′-Diiodo-4′-hydroxy-*N*-α-*tert*-butoxycarbonyl-D-phenylglycine ethylamide (**1a**), 3′,5′-diiodo-4′-hydroxy-*N*-α-*tert*-butoxycarbonyl-D-phenylglycine hexylamide (**1b**), 3′,5′-diiodo-4′-hydroxy-*N*-α-*tert*-butoxycarbonyl-D-phenylglycine laurylamide (**1c**), 3,5-diiodoaniline, 4-nitrosobenzonitrile, and 4-nitrosohexylbenzene were prepared according to the literature.[23,35–37] Monomers **2a–d** were newly synthesized according to Scheme 2. The details of the monomer synthesis and analytical and spectroscopic data are described in the Supporting Information. *N*,*N*-Dimethylformamide (DMF) and Et$_3$N used for polymerization were distilled prior to use.

Polymerization. All polymerizations were carried out in a glass tube equipped with a three-way stopcock under nitrogen. A typical experimental procedure for polymerization **1a** with **2a** is given below.

A solution of **1a** (164 mg, 0.30 mmol), **2a** (69.1 mg, 0.30 mmol), Pd(PPh$_3$)$_2$Cl$_2$ (4.2 mg, 6.0 μmol), CuI (6.9 mg, 36 μmol), PPh$_3$ (6.3 mg, 24 μmol), and Et$_3$N (0.6 mL) in DMF (0.9 mL) was stirred at 80 °C for 24 h. The resulting mixture was poured in MeOH/acetone [4/1 (v/v), 150 mL] to precipitate a polymer. It was separated by filtration using a membrane filter (ADVANTEC H020A047A) and dried under reduced pressure. The spectroscopic data of the polymer together with those of the other polymers are described in the Supporting Information.

RESULTS AND DISCUSSION

Monomer Synthesis and Sonogashira–Hagihara Coupling Polymerization. 3,5-Diethynylazobenzene monomers **2a–d** were synthesized by the route illustrated in Scheme 2. First, 3,5-diiodoazobenzene derivatives **3a–c** were synthesized by the condensation of 3,5-diiodoaniline with the corresponding nitrosobenzene derivatives in CH$_3$COOH. Compound **3d** was synthesized by the diazo coupling reaction of 3,5-diiodoaniline with phenol, followed by the formation of methyl etherification of 4-(3,5-diiodophenylazo)phenol because the reaction using 4-nitrosoanisole was unsatisfactory. Subsequently, the Sonogashira–Hagihara coupling reaction of **3a–d** with trimethylsilylacetylene and desilylation from the ethynyl group were carried out to obtain monomers **2a–d**. All monomers were characterized by ^{1}H, ^{13}C NMR, and IR spectroscopies besides elemental analysis or high-resolution mass spectrometry.

The Sonogashira–Hagihara coupling polymerization of **1a** with **2a**, **1b** with **2a–d**, and **1c** with **2a** was carried out in DMF at 80 °C for 24 h to obtain the corresponding polymers [poly(**1a–2a**)–poly(**1c–2a**)] with M_w values in the range of 6900–15 400 in 62–84% yields, as listed in Table 1.[38] Except for poly(**1b–2b**), the polymers were soluble in common organic solvents such as CH$_2$Cl$_2$, CHCl$_3$, THF, DMSO, and DMF. Poly(**1b–2b**) was insoluble in CH$_2$Cl$_2$ and CHCl$_3$ and partially soluble in THF, DMSO, and DMF.

Chiroptical Properties of the Polymers. The CD and UV–vis spectra of the polymers were measured in CH$_2$Cl$_2$ at

Table 1. Sonogashira–Hagihara Coupling Polymerization of 1a–c with 2a–d[a]

monomer		polymer		
		yield (%)[b]	M_w[c]	M_w/M_n[c]
1a+**2a**	poly(**1a**–**2a**)	83	11 900	1.9
1b+**2a**	poly(**1b**–**2a**)	62	15 400	1.8
1b+**2b**	poly(**1b**–**2b**)	65	8800[d]	1.5[d]
1b+**2c**	poly(**1b**–**2c**)	68	6900	1.8
1b+**2d**	poly(**1b**–**2d**)	84	14 000	1.9
1c+**2a**	poly(**1c**–**2a**)	72	10 900	1.6

[a] Conditions: [**1a**–**c**] = [**2a**–**d**] = 0.20 M, [$PdCl_2(PPh_3)_2$] = 0.0040 M, [CuI] = 0.024 M, [PPh_3] = 0.016 M, Et_3N/DMF = 2/3 (v/v), 80 °C, 24 h. [b] MeOH/acetone = 4/1 (v/v) insoluble part. [c] Determined by GPC eluted with $CHCl_3$, polystyrene calibration. [d] Eluted with THF.

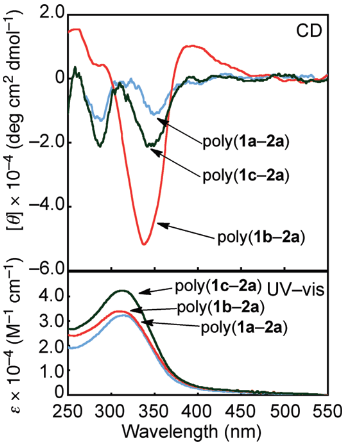

Figure 1. CD and UV–vis spectra of poly(**1a**–**2a**), poly(**1b**–**2a**), and poly(**1c**–**2a**) measured in CH_2Cl_2 (c = 0.030 mM) at 20 °C.

20 °C to obtain information on the secondary structures. Poly(**1a**–**2a**), poly(**1b**–**2a**), and poly(**1c**–**2a**) exhibited CD signals at 250–450 nm, as shown in Figure 1. They showed UV–vis absorption at the same region (λ_{max} around 315 nm) as the CD signals. The λ_{max} values of the polymers appeared red-shifted by 76–79 nm compared to those of **1a**–**c**. It is considered that these CD and UV–vis absorption peaks come from the conjugated *m*-phenyleneethynylene backbone. The absorption derived from the azobenzene moieties seems to overlap with that of the main chains because the λ_{max} of **2a** was 320 nm as well. Hence, it is considered that poly(**1a**–**2a**), poly(**1b**–**2a**), and poly(**1c**–**2a**) adopt helical conformations with predominantly one-handed screw sense in CH_2Cl_2 in a manner similar to the analogous poly(*m*-phenyleneethynylene-*p*-phenyleneethynylene)s.[23] The CD intensity of poly(**1c**–**2a**) was higher than that of poly(**1a**–**2a**) probably because of the longer alkyl chains, which are effective to stabilize the helical structure by enhancing the hydrophobicity of the helix exterior and/or hydrophobic interaction between the side chains.

It should be noted that the CD spectrum of poly(**1b**–**2a**) was different from those of poly(**1a**–**2a**) and poly(**1c**–**2a**). We filtered the sample solution using a membrane with a pore size of 0.45 μm and then measured the CD and UV–vis spectra of the sample again. Interestingly, the CD signal of poly(**1b**–**2a**) became nearly identical to those of the other two polymers, poly(**1a**–**2a**) and poly(**1c**–**2a**), as shown Figure 2. This result suggests that poly(**1b**–**2a**) formed the chiral aggregates exhibiting the different CD signals from those of nonaggregated states. Namely, it is likely that the intense chirality of the aggregates is induced by chiral arrangement of the chiral helical polymers. Because the UV–vis intensities of the sample before and after filtration were almost the same, it is likely that the population of the aggregates is very small. The CD and UV–vis spectra of poly(**1a**–**2a**) and poly(**1c**–**2a**) samples did not change at all before and after filtration.

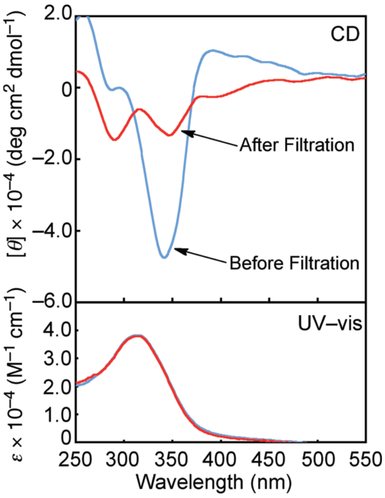

Figure 2. CD and UV–vis spectra of poly(**1b**–**2a**) measured in CH_2Cl_2 (c = 0.030 mM) at 20 °C before and after filtration using a membrane with 0.45 μm pore size.

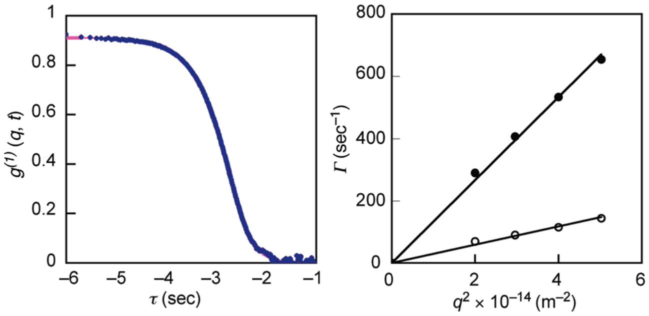

Figure 3. DLS results for solutions of poly(**1b**–**2a**) 0.10 wt % in CH_2Cl_2 measured at a scattering angle of 90° at 25 °C. Left: Time correlation functions for the scattered filed. Solid lines are double-exponential fits. Right: Decay rate Γ versus q^2 plot for poly(**1b**–**2a**) for the fast mode (●) and slow mode (○). The excellent linearity in this plot guarantees that both of these two modes correspond to the translational diffusion. The diffusion coefficients of the particles were evaluated from the slopes of the straight lines for the fast mode.

We measured the DLS of a CH_2Cl_2 solution of poly(**1b**–**2a**) to elucidate the formation of aggregates. From the correlation functions depicted in Figure 3, a hydrodynamic radius (R_h) could be evaluated from both fast and slow modes. From the fast mode, the presence of aggregated particles with an R_h around 385 nm was confirmed. The slow mode indicates the presence of very large aggregates whose size is ~2000 nm, which is larger by the order of magnitude. According to the scattering principle, the scattering intensity is proportional to the volume of the scatterer, and hence the number population of the large aggregates should be 10^{-3} or less, which leads us to the conclusion that the fast mode is the main

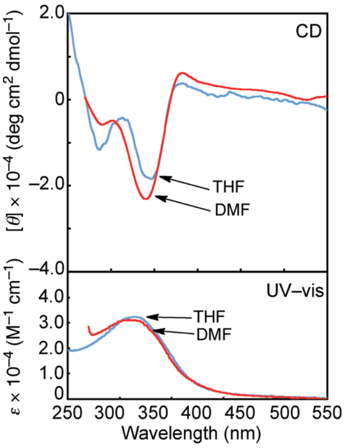

Figure 4. CD and UV–vis spectra of poly(**1b**–**2a**) measured in THF and DMF (c = 0.030 mM) at 20 °C.

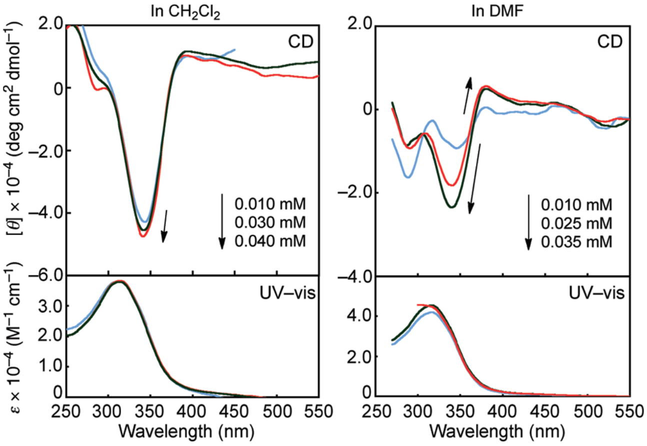

Figure 5. CD and UV–vis spectra of poly(**1b**–**2a**) measured in CH_2Cl_2 (left) and DMF (right) at various concentrations at 20 °C.

component, about which we should discuss. The filtration of the sample solution resulted in the disappearance of the DLS modes assignable to aggregated particles (fast mode) in addition to the large aggregates (slow mode). It is concluded that the aggregated particles have chirality, showing the intense CD signals.[39]

Figure 4 shows the CD and UV–vis spectra of poly(**1b**–**2a**) measured in THF and DMF. The previously reported hydroxyphenylglycine-based poly(*m*-phenyleneethynylene-*p*-phenyleneethynylene)s exhibited Cotton effect on the CD spectrum, indicating the formation of predominantly one-handed helical conformation in THF, whereas no CD signal was observed in DMF.[32] Poly(**1b**–**2a**), on the contrary, exhibited intense CD signals in either of the solvents. Poly(**1b**–**2a**) seems to have a high ability to form a chiral higher-order structure compared with the reported hydroxyphenylglycine-based poly(*m*-phenyleneethynylene-*p*-phenyleneethynylene)s. The all meta-linked structure of poly(**1b**–**2a**) may be preferable for the polymer to adopt a folded structure. In addition, the azobenzene moieties of poly(**1b**–**2a**) may participate in intramolecular π-stacking between the phenylene groups of the main chain, resulting in the high ability of helix formation. Poly(**1a**–**2a**) and poly(**1c**–**2a**) also exhibited CD signals in CH_2Cl_2, THF, and DMF (Figure S4 of the Supporting Information).

Table 2. Solution-State IR Spectroscopic Data (Amide and Carbamate C═O Absorption Peaks) of the Monomers and Polymers[a]

compound	wavenumber (cm^{-1})	
	amide C═O	carbamate C═O
1a	1683	1707
poly(**1a**–**2a**)	1654	1701
1b	1682	1707
poly(**1b**–**2a**)	1653	1701
1c	1682	1706
poly(**1c**–**2a**)	1654	1701

[a] Measured in CH_2Cl_2 (c = 10–20 mM).

As mentioned above, poly(**1b**–**2a**) formed chiral aggregates in CH_2Cl_2, whereas poly(**1a**–**2a**) and poly(**1c**–**2a**) did not. It is presumed that the chain length of alkyl groups of poly(**1b**–**2a**) match the requirement for inducing aggregation. The CD intensity slightly increased as the sample concentration was increased in CH_2Cl_2 as shown in Figure 5, left. An interesting phenomenon was observed in DMF, as shown in Figure 5, right. At a concentration of 0.010 mM, a nonaggregated CD pattern was observed. At 0.025 mM, an aggregated CD pattern appeared, and the intensity increased as the concentration was increased to 0.035 mM. It was confirmed that the critical aggregation concentration of poly(**1b**–**2a**) exists between 0.010 and 0.025 mM in DMF.

The helical structures of poly(*m*-phenyleneethynylene)s are commonly susceptible to temperature.[40,41] We measured the CD spectra of poly(**1a**–**2a**), poly(**1b**–**2a**), and poly(**1c**–**2a**) in CH_2Cl_2 at 0–40 °C to find negligibly small changes (Figure S5 of the Supporting Information). The Kuhn's dissymmetry factors ($g = \Delta\varepsilon/\varepsilon$, in which $\Delta\varepsilon = [\theta]/3298$) of poly(**1a**–**2a**) and poly(**1c**–**2a**) decreased only 6 and 5% by raising temperature from 20 to 40 °C, and that of poly(**1b**–**2a**) did not decreased at this temperature range.[42] The g values gives quantitative information associated with the degree of preferential screw sense.[43] The temperature dependence of g values of the present polymers is very small compared with that of the previously reported poly(*m*-phenyleneethynylene) derivatives. For example, the g value of a poly(phenyleneethynylene) tethering tetraethylene glycol decreases by 17% from 20 to 40 °C.[40]

Therefore, the higher-order structures of the polymers are thermally stable compared with the poly(*m*-phenyleneethynylene)s reported so far. This is explainable by the presence of intramolecular hydrogen bonding between the amide and carbamate groups at the side chains, which was confirmed by the solution state IR spectra of the polymers measured in CH_2Cl_2 at diluted concentrations (Table 2). The carbonyl absorption peaks of amide and carbamate groups of the polymers were observed at 28–29 and 5–6 cm^{-1} lower than those of the monomers **1a**–**c**, respectively.

Poly(**1b**–**2c**) and poly(**1b**–**2d**) also exhibited CD signals, as shown Figure 6, indicating that they also formed chiral higher-order structures. Poly(**1b**–**2b**) exhibited no CD signal in THF and DMF (Figure S6 of the Supporting Information). The electron-withdrawing character of the CN groups seems to affect the amphiphilic balance, preventing the polymer from adopting a helical conformation with predominantly one-handed screw sense.

Only poly(**1b**–**2a**) formed a chirally aggregated structure in CH_2Cl_2 among the polymers containing of monomer **1b** unit. This is probably because the affinity of poly(**1b**–**2a**) to CH_2Cl_2

is smaller than that of poly(**1b**−**2c**) and poly(**1b**−**2d**) having hexyl and methoxy groups, respectively. Poly(**1b**−**2c**) and poly(**1b**−**2d**) showed λ_{max} values longer than that of poly(**1b**−**2a**), as shown in Figure 6. Poly(**1b**−**2d**) showed the longest λ_{max}, corresponding to the λ_{max} order of the monomers (**2a**: 320 nm, **2c**: 335 nm, **2d**: 354 nm). This is quite reasonable because the π−π^* transition band of azobenzene is shifted to a longer wavelength region by introducing electron-donating groups.[44]

Figure 7 depicts the changes of CD and UV−vis spectra of poly(**1b**−**2a**), poly(**1b**−**2c**), and poly(**1b**−**2d**) with UV-light irradiation. The polymer solutions in CH_2Cl_2 were irradiated with a 400 W high-pressure mercury lamp through a suitable filter to exclude the light of the wavelength below 300 nm and above 400 nm. The UV−vis absorption of poly(**1b**−**2a**) at 320 nm decreased as UV-light irradiation, accompanying a decrease of CD intensity at 340 nm, and took photostationary state after 8 min. These spectroscopic changes indicate that the *trans*-azobenzene moieties isomerized into cis form, resulting in partial collapse of a chirally aggregated structure. It seems that the bended main chain of photoirradiated poly(**1b**−**2a**) due to the *cis*-azobenzene moieties is unfavorable for aggregation compared with the more linear main chain before irradiation. No absorption attributable to n−π^* transition of *cis*-azobenzene unit was observed around 440 nm probably because of the low photoisomerization ratio, which was estimated to be 7% based on change of the UV−vis absorption.[45] The low degree of photoisomerization is attributable to the overlap of π−π^* transition band of the phenyleneethynylene main chain with that of the *trans*-azobenzene units.[19] It is considered that the UV-light was absorbed not only by the azobenzene units but also by the conjugated main chain, preventing the effective photoisomerization. This assumption seems to be reasonable from the photoisomerization data of poly(**1b**−**2c**) and poly(**1b**−**2d**). Namely, it was calculated that the trans → cis isomerization ratios of azobenzene units of poly(**1b**−**2c**) and poly(**1b**−**2d**) were 17 and 31%, respectively, which were higher than that of poly(**1b**−**2a**). As mentioned above, the π−π^* transition bands of azobenzene moieties of poly(**1b**−**2c**) and poly(**1b**−**2d**) are positioned at longer wavelength regions than that of poly(**1b**−**2a**). It is considered that the azobenzene moieties of the former two polymers can absorb UV-light with higher efficiencies because the overlaps of the absorption bands with those of phenyleneethynylene backbones are smaller. Interestingly, the CD signals of poly(**1b**−**2c**) and poly(**1b**−**2d**) around 450 nm increased with UV-light irradiation. This result suggests that the polymers induced a certain regulated structure according to the photoisomerization of the azobenzene moieties. Visible-light irradiation to the UV-light irradiated samples resulted in complete recovery of the initial CD and UV−vis spectroscopic patterns. Reversible conformational changes were confirmed in all polymers.

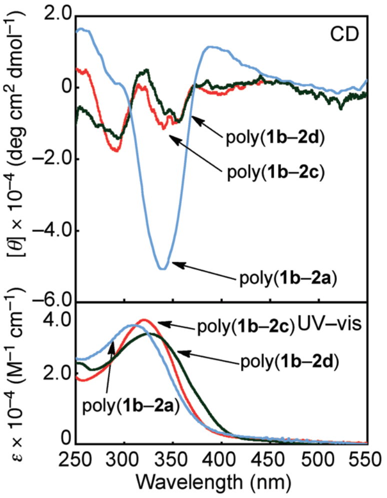

Figure 6. CD and UV−vis spectra of poly(**1b**−**2a**), poly(**1b**−**2c**), and poly(**1b**−**2d**) measured in CH_2Cl_2 (c = 0.030 mM) at 20 °C. Poly(**1b**−**2b**) was insoluble in CH_2Cl_2.

Chart 1. Structure of 18-mers of Poly(1a−2a)[a]

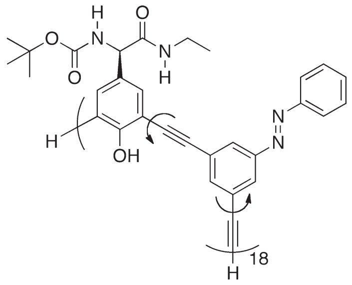

[a] Arows indicate a torsional angle per phenylene unit.

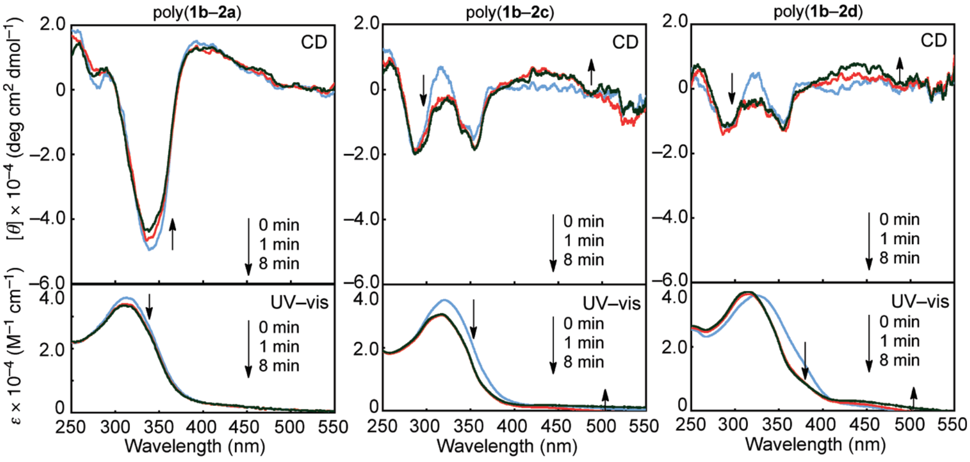

Figure 7. CD and UV−vis spectra of poly(**1b**−**2a**) (left), poly(**1b**−**2c**) (center), and poly(**1b**−**2d**) (right) measured in CH_2Cl_2 (c = 0.030 mM) with irradiation at 300 < λ < 400 nm at 20 °C.

Chart 2. Possible Regulated Conformers of Poly(1a−2a)-18-mer[a]

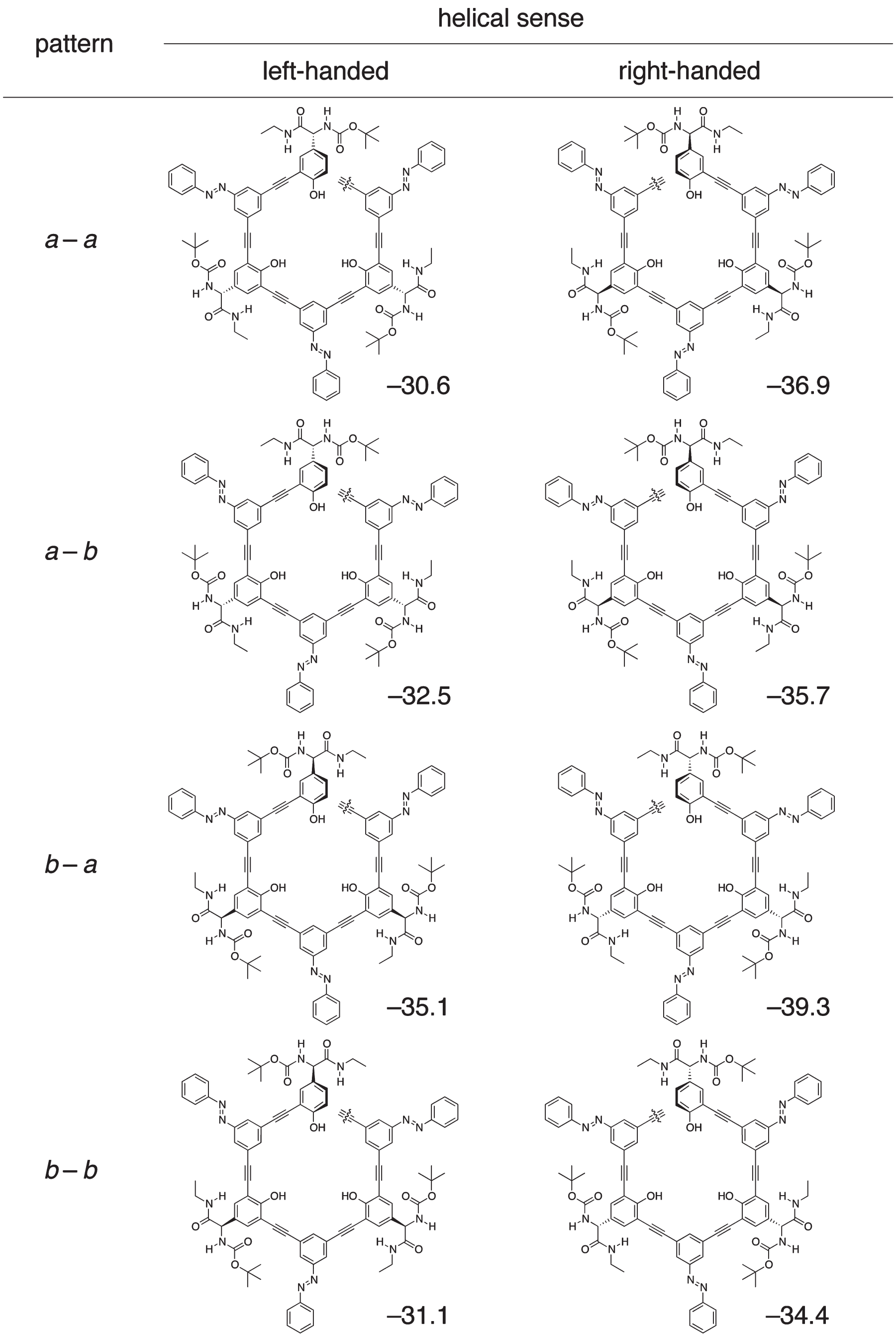

[a] Fifteen monomer units are omitted at the wavy lines. The values are the energies in kJ/mol·unit of the conformers after geometry optimization by the MMFF94 method.

Conformational Analysis. The conformations of poly(*m*-phenyleneethynylene)s have been analyzed by several methods because they have been found to fold into helices under certain conditions. Amine-[46,47] and ester-functionalized[48] poly(*m*-phenyleneethynylene)s energetically prefer helical conformations to coiled and extended ones in water, wherein surrounding water molecules play an important role to fold the polymer chains according to the molecular dynamics simulations. When the molecule adopts a helical conformation, the interaction between the polar side chains and solvents becomes maximum and π-stacking interaction between phenylene units as well. The unfavorable contact between the hydrocarbon backbone and polar solvents becomes minimum simultaneously.[1b]

Judging from the nature of poly(*m*-phenyleneethynylene)s, it is likely that the polymers in the present study also adopt folded helical structures with stacked phenylene moieties. We examined the conformation of the polymers based on the molecular mechanics method (MMFF94).[49] We first constructed helical 18-mers of poly(**1a**−**2a**), whose both chain ends were terminated with hydrogen atoms, as illustrated in Chart 1. The torsional angles of main chains of left- and right-handed helices were set to −6 and +6° per phenylene unit at the initial geometries, respectively.

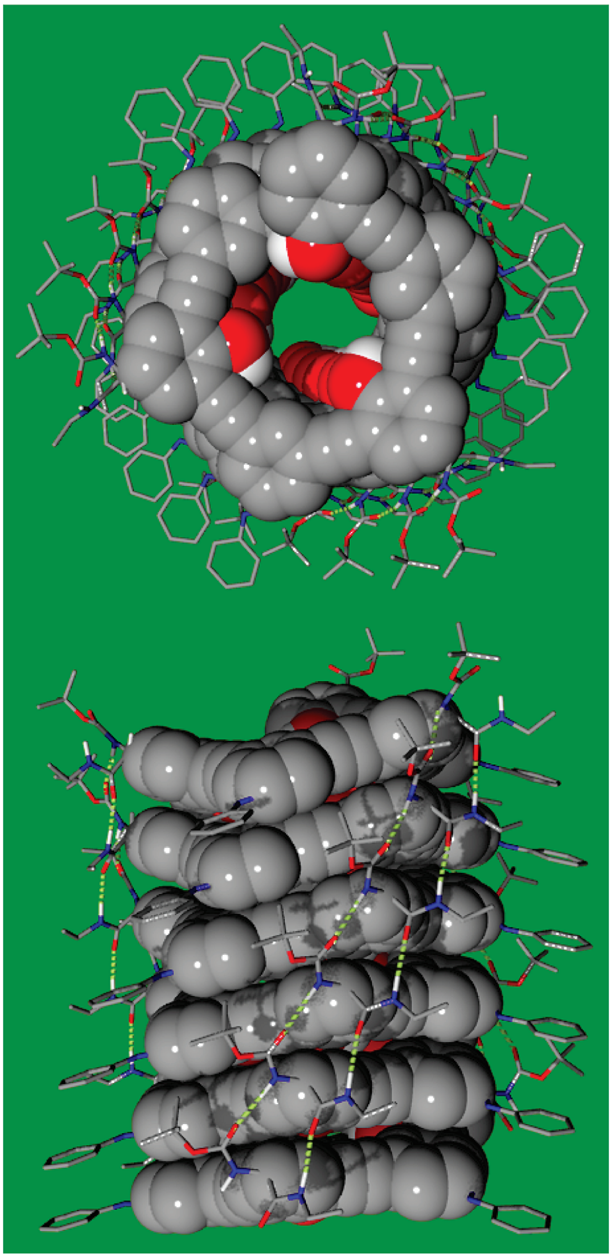

Figure 8. Top and side views of a possible conformation (right-handed *b*−*a* in Chart 2) of poly(**1a**−**2a**)-18-mer. The phenyleneethynylene main chain and O−H groups are illustrated by the space filling models, and the hydrogen atoms other than N−H and O−H moieties are omitted for enhancement of visibility. The green dotted lines represent hydrogen bonds (N−H···O═C) between the amide groups and carbamate groups. Geometries were optimized by the MMFF94 method.

Chart 2 illustrates the eight possible regulated conformers. Symbols *a* and *b* in the pattern column represent the two ways of directions (+180° and −180°) of the carbamate/amide and azobenzene moieties along the conjugated plane of the main chain.

After geometry optimization, the right-handed helical 18-mers became 3.2−6.3 kJ/mol·unit more stable than the left-handed counterparts of patterns *a*−*a*, *a*−*b*, *b*−*a*, and *b*−*b*. Among the eight conformers, the right-handed *b*−*a* in Chart 2 was the most stable. As shown in Figure 8, the amide and carbamate N−H groups of a monomer unit formed regulated intramolecular hydrogen bonds with the C═O groups of the amide and carbamate groups three units earlier ($i + 3 \rightarrow i$ N−H···O═C hydrogen bonding), respectively. Accordingly, the conformer is surrounded by regulated three hydrogen-bonding strands formed at the amide groups, and the other three hydrogen-bonding strands formed at the carbamate groups. The interatomic distances of the hydrogen and oxygen (N−H···O═C) participating in hydrogen bonding between the ($i + 3$)th and *i*th units at the amide and carbamate moieties were 1.76 and 1.79 Å on average, respectively. The shorter interatomic distance between the amide groups may explain the larger shift of carbonyl absorption of the solution state IR from the monomer to polymer than that of carbamate as listed in Table 2. The hydroxy groups inside the helix cannot hydrogen bond each other because the distance is too long (3 to 4 Å). The helical pitch after geometry optimization was 3.8 Å, which was the same as the value before optimization. This value is consistent with the turns of the helix being near van der Waals contact and comparable to π-stacking between aromatic rings.[47]

CONCLUSIONS

In this Article, we have demonstrated the synthesis of novel photoresponsive optically active poly(*m*-phenyleneethynylene)s by the Sonogashira−Hagihara coupling polymerization of D-phenylglycine-derived *m*-diiodobenzenes with 3,5-diethynylazobenzene derivatives. CD and UV−vis spectroscopic studies revealed that the polymers except for poly(**1b**−**2b**) formed thermally stable chiral higher-order structures in CH_2Cl_2, THF, and DMF. Unlike the reported poly(*m*-phenyleneethynylene)s, the present polymers could form chiral higher-order structures in nonpolar CH_2Cl_2 and in polar DMF as well. The presence of intramolecular hydrogen bonds between the amide and carbamate groups at the side chains seems to be effective to stabilize the higher-order structures. The *trans*-azobenzene moieties of the polymers isomerized into cis forms upon UV-light irradiation, accompanying the conformational changes of the polymers. Poly(**1b**−**2a**) formed a chirally aggregated structure in CH_2Cl_2, which partially collapsed according to trans → cis photoisomerization. Poly(**1b**−**2c**) and poly(**1b**−**2d**) showed other CD signals at regions of n−π^* transition band of *cis*-azobenzene moieties after UV-light irradiation, indicating the formation of chiral structures different from those before photoirradiation. The degree of photoisomerization was improved by introducing a para-substituent in the azobenzene. The azobenzene moieties of the polymers reversibly isomerized from cis to trans upon visible-light irradiation, recovering the initial higher-order structures.

ASSOCIATED CONTENT

Ⓢ Supporting Information. Experimental procedure for monomer synthesis, analytical, and spectroscopic data of the monomers and polymers, ^{1}H NMR spectrum of **2a** (Figure S1), ^{1}H NMR spectrum of poly(**1b**−**2a**) (Figure S2), DLS results for poly(**1a**−**2a**) and poly(**1c**−**2a**) (Figure S3), CD and UV−vis spectra of poly(**1a**−**2a**) and poly(**1c**−**2a**) (Figure S4), plots of *g* of poly(**1a**−**2a**), poly(**1b**−**2a**), and poly(**1c**−**2a**) at 0−40 °C (Figure S5), and CD and UV−vis spectra of poly(**1b**−**2b**) (Figure S6). This material is available free of charge via the Internet at http://pubs.acs.org.

AUTHOR INFORMATION

Corresponding Author

*E-mail: sanda@adv.polym.kyoto-u.ac.jp.

■ ACKNOWLEDGMENT

This research was supported by a Grant-in-Aid for Science Research (B) (22350049) and Kyoto University Global COE Program "International Center for Integrated Research and Advanced Education in Materials Science" from the Ministry of Education, Culture, Sports, Science, and Technology, Japan, and The Kurata Memorial Hitachi Science and Technology Foundation. We are grateful to Mr. Tomoyuki Ohnishi at Kyoto University for measurement of DLS.

■ REFERENCES

(1) Reviews: (a) Yashima, E.; Maeda, K.; Iida, H.; Furusho, Y.; Nagai, K. *Chem. Rev.* **2009**, *109*, 6102–6211. (b) Hill, D. J.; Mio, M. J.; Prince, R. B.; Hughes, T. S.; Moore, J. S. *Chem. Rev.* **2001**, *101*, 3893–4011. (c) Nakano, T.; Okamoto, Y. *Chem. Rev.* **2001**, *101*, 4013–4038.

(2) Reviews: (a) David, B. A.; Serrano, J.; Sierra, T.; Veciana, J. *J. Polym. Sci., Part A: Polym. Chem.* **2006**, *44*, 3161–3174. (b) Suginome, M.; Ito, Y. *Adv. Polym. Sci.* **2004**, *171*, 77–136. (c) Cornelissen, J. J. L. M.; Rowan, A. E.; Nolte, R. J. M.; Sommerdijk, N. A. J. M. *Chem. Rev.* **2001**, *101*, 4039–4070.

(3) Reviews: (a) Shiotsuki, M.; Sanda, F.; Masuda, T. *Polym. Chem.*, in press. DOI: 10.1039/c0py00333f. (b) Masuda, T. *J. Polym. Sci., Part A: Polym. Chem.* **2007**, *45*, 165–180. (c) Aoki, T.; Kaneko, T.; Teraguchi, M. *Polymer* **2006**, *47*, 4867–4892.

(4) Reviews: (a) Kane-Maguire, L. A. P.; Wallace, G. G. *Chem. Soc. Rev.* **2010**, *39*, 2545–2576. (b) Hoeben, F. J. M.; Jonkheijim, P.; Meijer, E. W.; Schenning, A. P. H. J. *Chem. Rev.* **2005**, *105*, 1491–1546.

(5) Review: Ajayaghosh, A.; Praveen, V. K. *Acc. Chem. Res.* **2007**, *40*, 644–656.

(6) Reviews: (a) Bunz, U. H. F. *Macromol. Rapid Commun.* **2009**, *30*, 772–805. (b) Smaldone, R. A.; Moore, J. S. *Chem.—Eur. J.* **2008**, *14*, 2650–2657. (c) Bunz, U. H. F. *Adv. Polym. Sci.* **2005**, *177*, 1–52.

(7) Fukuhara, G.; Inoue, Y. *J. Am. Chem. Soc.* **2011**, *133*, 768–770.

(8) Tamura, K.; Miyabe, T.; Iida, H.; Yashima, E. *Polym. Chem.* **2011**, *2*, 91–98.

(9) Fukuhara, G.; Inoue, Y. *Chem.—Eur. J.* **2010**, *16*, 7859–7864.

(10) Smaldone, R. A.; Moore, J. S. *J. Am. Chem. Soc.* **2007**, *129*, 5444–5450.

(11) Ikeda, M.; Furusho, Y.; Okoshi, K.; Tanahara, S.; Maeda, K.; Nishio, S.; Mori, T.; Yashima, E. *Angew. Chem., Int. Ed.* **2006**, *45*, 6491–6495.

(12) Abe, H.; Masuda, N.; Waki, M.; Inouye, M. *J. Am. Chem. Soc.* **2005**, *127*, 16189–16196.

(13) Yamamoto, T.; Yamada, T.; Nagata, Y.; Suginome, M. *J. Am. Chem. Soc.* **2010**, *132*, 7889–7901.

(14) Terada, K.; Masuda, T.; Sanda, F. *J. Polym. Sci., Part A: Polym. Chem.* **2009**, *47*, 2596–2602.

(15) Maeda, K.; Tanaka, K.; Morino, K.; Yashima, E. *Macromolecules* **2007**, *40*, 6783–6785.

(16) Kakuchi, R.; Shimada, R.; Tago, Y.; Sakai, R.; Satoh, T.; Kakuchi, T. *J. Polym. Sci., Part A: Polym. Chem.* **2010**, *48*, 1683–1689.

(17) Kakuchi, R.; Kodama, T.; Shimada, R.; Tago, Y.; Sakai, R.; Satoh, T.; Kakuchi, T. *Macromolecules* **2009**, *42*, 3892–3897.

(18) Thomas, S. W, III; Joly, G. D.; Swager, T. M. *Chem. Rev.* **2007**, *107*, 1339–1386.

(19) Li, C.; Guo, Y.; Lv, J.; Xu, J.; Li, Y.; Wang, S.; Liu, H.; Zhu, D. *J. Polym. Sci., Part A: Polym. Chem.* **2007**, *45*, 1403–1412.

(20) Zhao, X.; Schanze, K. S. *Langmuir* **2006**, *22*, 4856–4862.

(21) Arnt, L.; Tew, G. N. *Macromolecules* **2004**, *37*, 1283–1288.

(22) Liu, R.; Sogawa, H.; Shiotsuki, M.; Masuda, T.; Sanda, F. *Polymer* **2010**, *51*, 2255–2263.

(23) Liu, R.; Shiotsuki, M.; Masuda, T.; Sanda, F. *Macromolecules* **2009**, *42*, 6115–6122.

(24) Reviews: (a) Seki, T. *Bull. Chem. Soc. Jpn.* **2007**, *80*, 2084–2109. (b) Natansohn, A.; Ronchon, P. *Chem. Rev.* **2002**, *102*, 4139–4175. (c) Tamai, N.; Miyasaka, H. *Chem. Rev.* **2000**, *100*, 1875–1890.

(25) Ercole, F.; Davis, T. P.; Evans, R. A. *Polym. Chem.* **2010**, *1*, 37–54.

(26) Stoll, R. S.; Peters, M. V.; Kuhn, A.; Helices, S.; Goddard, R.; Buhl, M.; Thiele, C. M.; Hecht, S. *J. Am. Chem. Soc.* **2009**, *131*, 357–367.

(27) Masiero, S.; Lena, S.; Pieraccini, S.; Spada, G. P. *Angew. Chem., Int. Ed.* **2008**, *47*, 3184–3187.

(28) Yamada, M.; Kondo, M.; Mamiya, J.; Yu, Y.; Kinoshita, M.; Barrett, C. J.; Ikeda, T. *Angew. Chem., Int. Ed.* **2008**, *47*, 4986–4988.

(29) Koumura, N.; Kudo, M.; Tamoki, N. *Langmuir* **2004**, *20*, 9897–9990.

(30) Furusho, Y.; Tanaka, Y.; Maeda, T.; Ikeda, M.; Yashima, E. *Chem. Commun.* **2007**, 3174–3176.

(31) Fujii, T.; Shiotsuki, M.; Inai, Y.; Sanda, F.; Masuda, T. *Macromolecules* **2007**, *40*, 7079–7088.

(32) Khan, A.; Hecht, S. *Chem.—Eur. J.* **2006**, *12*, 4764–4774.

(33) Zhao, H.; Sanda, F.; Masuda, T. *Polymer* **2006**, *47*, 2596–2602.

(34) Mayer, S.; Zentel, R. *Prog. Polym. Sci.* **2001**, *26*, 1973–2013.

(35) Bérubé, M.; Poirier, D. *Org. Lett.* **2004**, *6*, 3127–3130.

(36) ten Brink, G.; Vis, J. M.; Arends, I. W. C. E.; Sheldon, R. A. *Tetrahedron* **2002**, *58*, 3977–3983.

(37) Anspon, H. D. *Org. Synth.* **1955**, *3*, 711–712.

(38) We measured the ^{13}C NMR spectrum of poly(**1b**–**2a**) in CDCl$_3$ (50 mM) to confirm the purity of the polymer chain. One broad signal assignable to $-C{\equiv}C-$ was observed around 80.1 ppm. No peak assignable to $-C{\equiv}C-C{\equiv}C-$ was observed around 74 ppm (e.g., $Ph-C{\equiv}C-C{\equiv}C-Ph$ 74.2 ppm). Consequently, it is concluded that oxidative acetylene coupling, a typical side reaction of the Sonogashira–Hagihara coupling, does not take place during the polymerization, and the present polymer does not contain diacetylene units. The relatively low molecular weights of the polymers may be caused by a small deviation from equivalency between the diiode monomers and diyne monomers due to the small scale of the polymerization (0.30 mmol).

(39) The DLS measurements were also performed for CH$_2$Cl$_2$ solutions (0.1 wt %) of poly(**1a**–**2a**) and poly(**1c**–**2a**) (Figure S3 of the Supporting Information). Particles with R_h values of 585 and 477 nm were detected, respectively. These two polymers also seem to form aggregates at this concentration. On the contrary, these two polymers did not show the CD signals in CH$_2$Cl$_2$ [$c = 0.030$ mM ((1.24 to 1.56) $\times 10^{-3}$ wt %)] attributable to the aggregates. It is presumed that this is due to the difference in sample concentrations between DLS and CD measurements. The concentrations of the DLS samples were 65–80 times higher than those of the CD samples. Because of the different requirements of sample concentrations, we could not obtain the data of DLS and CD at the same concentration.

(40) Prince, R. B.; Brunsyeld, L.; Meijer, E. W.; Moore, J. S. *Angew. Chem., Int. Ed.* **2000**, *39*, 228–230.

(41) Prince, R.; Saven, J. G.; Wolynens, P. G.; Moore, J. S. *J. Am. Chem. Soc.* **1999**, *121*, 3114–3121.

(42) Aggregation also seems to contribute to the thermal stability in the case of poly(**1b**–**2a**).

(43) Fujiki, M. *Macromol. Rapid Commun.* **2001**, *22*, 539–563.

(44) Gore, P. R.; Wheeler, O. H. *J. Org. Chem.* **1961**, *26*, 3295–3298.

(45) Moniruzzaman, M.; Talbot, J. D. R.; Sabey, C. J.; Fernando, G. F. *J. Appl. Polym. Sci.* **2006**, *100*, 1103–1112.

(46) Adisa, B.; Bruce, D. A. *J. Phys. Chem. B* **2005**, *109*, 7548–7556.

(47) Adisa, B.; Bruce, D. A. *J. Phys. Chem. B* **2005**, *109*, 19952–19959.

(48) Lee, O. S.; Saven, J. G. *J. Phys. Chem. B* **2004**, *108*, 11988–11994.

(49) Halgren, T. A. *J. Comput. Chem.* 1996, 17, 490–519. The molecular mechanics calculation was carried out with Wavefunction, Inc., Spartan '08 Macintosh.